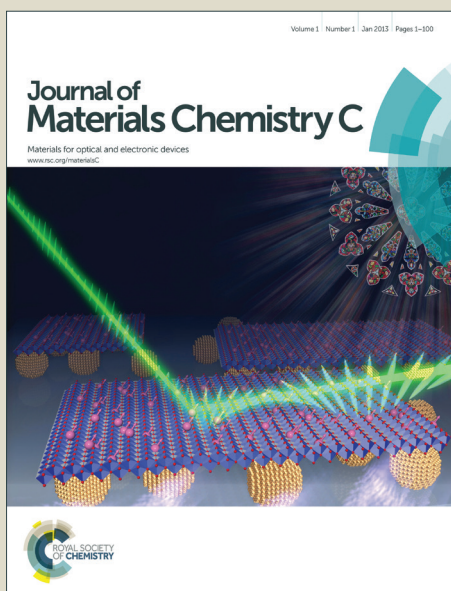


Journal of Materials Chemistry C

Accepted Manuscript



This is an *Accepted Manuscript*, which has been through the Royal Society of Chemistry peer review process and has been accepted for publication.

Accepted Manuscripts are published online shortly after acceptance, before technical editing, formatting and proof reading. Using this free service, authors can make their results available to the community, in citable form, before we publish the edited article. We will replace this *Accepted Manuscript* with the edited and formatted *Advance Article* as soon as it is available.

You can find more information about *Accepted Manuscripts* in the [Information for Authors](#).

Please note that technical editing may introduce minor changes to the text and/or graphics, which may alter content. The journal's standard [Terms & Conditions](#) and the [Ethical guidelines](#) still apply. In no event shall the Royal Society of Chemistry be held responsible for any errors or omissions in this *Accepted Manuscript* or any consequences arising from the use of any information it contains.

Interplay of Alternative Conjugated Pathways and Steric Interactions on the Electronic and Optical Properties of Donor-Acceptor Conjugated Polymers

Igo T. Lima,^{1,2} Chad Risko,^{1,†,*} Saadullah G. Aziz,³
Demétrio A. da Silva Filho,^{2,*} and Jean-Luc Brédas^{1,3,‡,*}

¹ School of Chemistry and Biochemistry and Center for Organic Photonics and Electronics
Georgia Institute of Technology
Atlanta, Georgia, 30332-0400, United States of America

² Institute of Physics, University of Brasilia, 70919-970, Brasilia, Brazil

³ Department of Chemistry, King Abdulaziz University, Jeddah 21589, Kingdom of Saudi Arabia

[†]*New Permanent Address:* Department of Chemistry, University of Kentucky, Lexington, Kentucky, 40506, USA

[‡]*New Permanent Address:* Physical Sciences and Engineering Division, King Abdullah University of Science and Technology (KAUST), Thuwal 23955-6900, Kingdom of Saudi Arabia

KEYWORDS. Donor-acceptor copolymers, orthogonal and linear conjugation, long-range corrected density functionals.

ABSTRACT

Donor-acceptor π -conjugated copolymers are of interest for a wide range of electronic applications, including field-effect transistors and solar cells. Here, we present a density functional theory (DFT) study of the impact of varying the conjugation pathway on the geometric, electronic, and optical properties of donor-acceptor systems. We consider both the linear (“in series”), traditional conjugation among the donor-acceptor moieties versus structures where the acceptor units are appended orthogonally to the linear, donor-only conjugated backbone. Long-range-corrected hybrid functionals are used in the investigation with the values of the tuned long-range separation parameters providing an estimate of the extent of conjugation as a function of the oligomer architecture. Considerable differences in the electronic and optical properties are determined as a function of the nature of the conjugation pathway, features that should be taken into account in the design of donor-acceptor copolymers.

INTRODUCTION

π -Conjugated molecules and polymers composed of donor (D, electron rich) and acceptor (A, electron poor) moieties have attracted considerable attention as the active materials in organic-based optoelectronic devices, such as field-effect transistors and organic solar cells.¹⁻¹³ Coupling donor moieties with a small ionization potential IP (*i.e.*, energetically destabilized HOMO level) to acceptor units with a large electron affinity EA (*i.e.*, energetically stabilized LUMO level) is a well-established means to tailor the redox and optical properties of thin-film molecule/polymer-based materials.¹⁴⁻¹⁸ Most systems in this materials class employ a structural motif where the donor and acceptor units are linked in a linear fashion, *i.e.*, -D-A-D-A-D-A-, or some variant thereof (Figure 1). Recently, orthogonally conjugated structures –where the acceptor (or donor) is appended to the side of the main, conjugated backbone– have been introduced as an alternative strategy.¹⁹⁻²² For instance, Zhang and co-workers showed that manipulating the electron-withdrawing strength of the acceptor groups attached to a backbone consisting of carbazole (Cz) and thiophene (Th) units, allowed the redox and optical properties to be effectively tuned.²¹ In addition, Grimm and co-workers, using oligomers and copolymers comprised of cyclopentadithiophene (CPDT) with an imine functionality appended to the CPDT bridgehead position,²³ demonstrated how orthogonal conjugation can lead to systems with low-energy (long wavelength) optical transitions, though the oscillator strengths (transition dipole moments) for these transitions tend to be smaller.

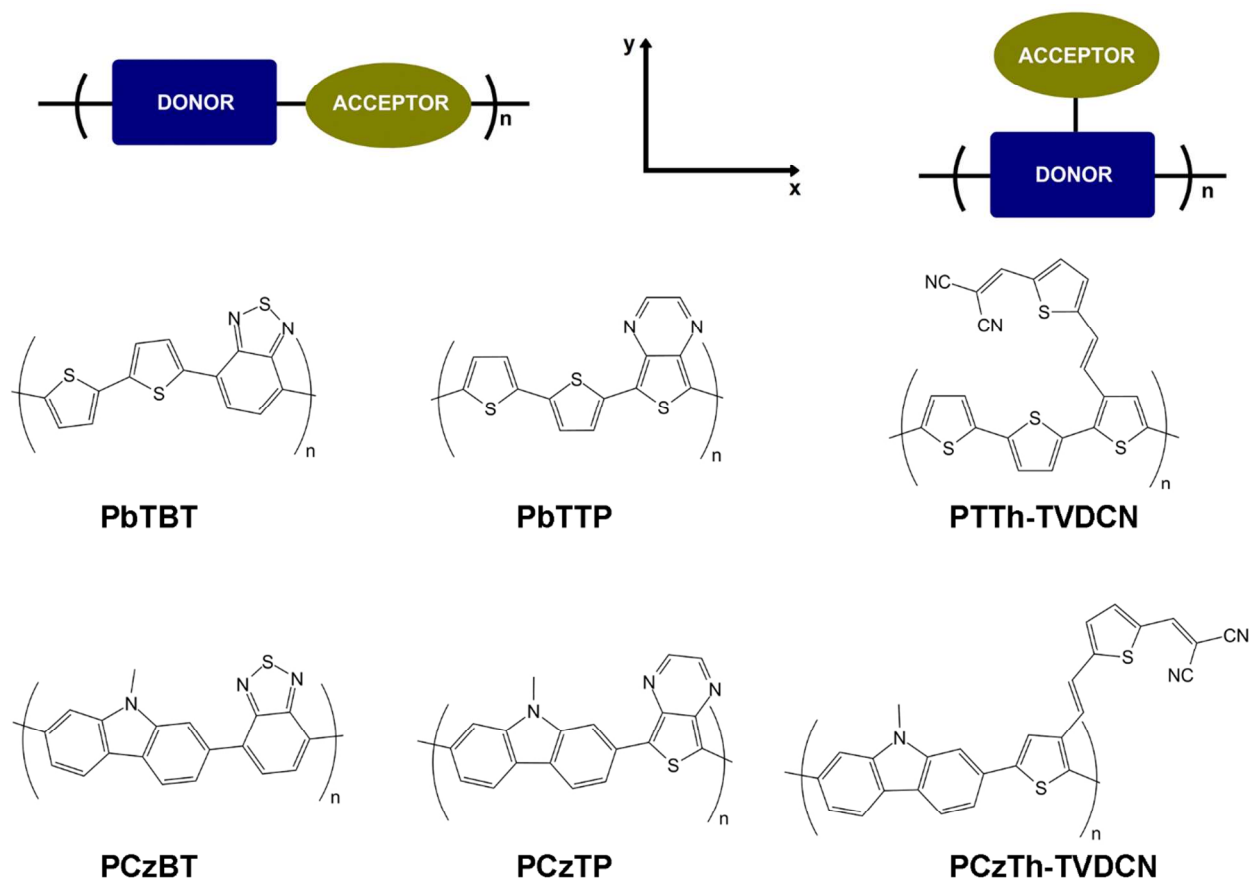


Figure 1. Chemical structures of the repeat units for: PbTBT \equiv poly[4-methyl-7-(5'-methyl-[2,2'-bithiophen]-5-yl)benzo[c][1,2,5]thiadiazole]; PbTTP \equiv poly[5-methyl-7-(5'-methyl-[2,2'-bithiophen]-5-yl)thieno[3,4-b]pyrazine]; PCzBT \equiv poly[4-(7,9-dimethyl-9H-carbazol-2-yl)-7-methylbenzo[c][1,2,5]thiadiazole]; PCzTP \equiv poly[5-(7,9-dimethyl-9H-carbazol-2-yl)-7-methylthieno[3,4-b]pyrazine]; PCzTh-TVDCN \equiv poly[(E)-2-((5-(2-(5-(7,9-dimethyl-9H-carbazol-2-yl)-2-methylthiophen-3-yl)vinyl)thiophen-2-yl)methylene)malononitrile]; and PTh-TVDCN \equiv poly[(E)-2-((5-(2-(5,5''-dimethyl-[2,2':5',2''-terthiophen]-3-yl)vinyl)thiophen-2-yl)methylene)malononitrile].

If such alternative conjugated pathways are to find broad use in materials applications, it is important to establish how the electronic and optical properties manifest as a function of such structural variations of the conjugation. In this work, we employ density functional theory (DFT) to investigate a systematic series of linear and orthogonally conjugated DA structures (see Figure 1) to establish a broad comparison of the geometric, electronic, and optical properties.^{9, 11, 21}

Here, carbazole (Cz) and bithiophene (Th) moieties are used as the donor groups, while three acceptor units were used to study the effects of the linear [benzothiadiazole (BT) and thienopyrazine (TP)] and orthogonal [thienylene-vinylene di-cyano (TVDCN)] conjugation pathways.²¹ These acceptor units were specifically chosen to be consistent with linear and orthogonal donor-acceptor copolymers reported in the literature.

COMPUTATIONAL METHODOLOGY

To model the DA copolymers, we considered oligomers with length $n = 1-4$, *i.e.*, from monomer to tetramer. The ground-state oligomer geometries were initially optimized via density functional theory (DFT) with the global hybrid B3LYP functional²⁴⁻²⁶ and a 6-31G(d,p) basis set.^{27, 28} We note that the longest oligomers ($n = 4$) present a linear conjugation pathway along the backbone of 24 double bonds, a conjugation length that has been shown to be long enough to produce accurate trends concerning the electronic and optical properties of DA copolymers.^{11, 23, 29, 30}

Conventional semi-local and standard hybrid DFT functionals, due to the limitations associated with multi-electron self-interaction errors, can lead to poor descriptions of the charge-transfer-like excitations expected in DA systems.^{31, 32} To overcome these limitations, we employ long-range-corrected hybrid functionals where the long-range separation parameter ω is tuned through the gap-fitting procedure proposed by Baer and Kronik.³³⁻³⁵

$$J_{IP}(\omega) = \left| \varepsilon_H^\omega(N) + E_{gs}^\omega(N-1) - E_{gs}^\omega(N) \right| \quad (1)$$

$$J_{EA}(\omega) = \left| \varepsilon_H^\omega(N+1) + E_{gs}^\omega(N) - E_{gs}^\omega(N+1) \right| \quad (2)$$

$$J_{gap}(\omega) = \sqrt{(J_{IP}(\omega))^2 + (J_{EA}(\omega))^2} \quad (3)$$

Here, $\varepsilon_H^\omega(N)$ is the HOMO energy for an N-electron system and $E_{gs}^\omega(N)$ the corresponding SCF energy. Analogously, $\varepsilon_H^\omega(N+1)$ is the SOMO (singly occupied molecular orbital) energy for an N+1-electron system and $E_{gs}^\omega(N+1)$ and $E_{gs}^\omega(N-1)$ are the corresponding SCF energies of the anion and cation states, respectively. Starting from the optimized B3LYP/6-31G(d,p) structure, both the long-range separation parameter ω of the LC-BLYP functional and the geometry were iteratively optimized to guarantee that the HOMO-LUMO gap obtained from the optimized functional is directly comparable to the fundamental gap; notably, the tuned LC-BLYP functional has been shown to produce results that correlate well with the properties of both linearly and orthogonally conjugated polymers.²³

The central idea surrounding the use of range-separated functionals for molecules is to partition the Coulomb operator into a short-range (SR) component, where a semilocal exchange-correlation functional is often used, and a long-range (LR) component, where the exchange part is treated at the exact nonlocal Hartree-Fock level. This approach allows one both to take advantage of the strengths of the semilocal approximations to the exchange-correlation functional and to minimize their shortcomings.³⁶ The range separation is usually introduced through use of the error function (*erf*):

$$\frac{1}{r} = \frac{\text{erf}(\omega r)}{r} + \frac{\text{erfc}(\omega r)}{r} \quad (4)$$

with the value of ω determining the distance where the description switches from SR to LR. Importantly, the optimal value of the range-separation parameter has been shown to be sensitive to the system under consideration,^{30, 37} with the ω tuning procedure introduced by Baer and

Kronik (and used here) showing improvements in the description of the electronic and optical properties of atomic and molecular systems (*e.g.*, the fundamental gap) and in particular charge-transfer excitations.³³⁻³⁵

Low-lying singlet excited states were evaluated with the iteratively tuned LC-BLYP/6-31G(d,p) optimized geometries using time-dependent density functional theory (TDDFT). Optical absorption profiles were simulated through convolution of the vertical transition energies with Gaussian functions with a full width at half-maximum (FWHM) equal to 0.3 eV. All calculations were performed with the Gaussian 09 (Rev.A.02 and B.01) code.³⁸

RESULTS AND DISCUSSION

a) Geometric Structure and Degree of Conjugation

We begin our analysis by discussing the ground-state geometric properties as a function of the nature of the donor and acceptor units. As might be expected, the relative degree of planarity along the main conjugated backbone is determined by the architecture of the donor and acceptor units. Figure 2 and Table 1 provide definitions and collect representative torsion angles (for tetramers) along the main conjugated backbone. For the linear DA oligomers, the steric interactions induced by the phenylene protons *ortho* to the carbazole-acceptor linkage lead to larger torsions along the backbone as compared to the very planar thiophene-thiophene-linked systems. Importantly, the pendant TVDCN groups in the orthogonally DA conjugated structures, even though they are appended to the side of the main conjugated backbone, lead to an even

larger degree of backbone twisting: The hydrogen atoms on the di-cyano group and the nearest-neighbor hydrogen atoms on the backbone are separated by 2.23 Å in PCzTh-TVDCN and 2.30 Å in PThTh-TVDCN, steric relief that arises through twisting along the backbone.

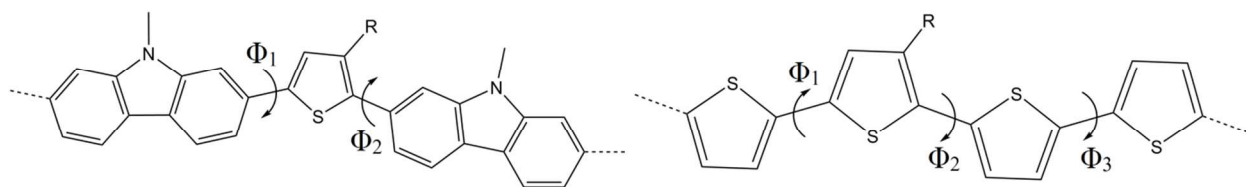


Figure 2. Definition of the torsion angles along the conjugated backbone of the DA oligomers.

Table 1. Torsion angles ($^{\circ}$) along the conjugated backbone of the tetramers.

Tetramers	Φ_1	Φ_2	Φ_3
PbTBT	0-1	0	0-1 (11)
PbTTP	0	0	0 (8)
PCzBT	29-30	29	-
PCzTP	0-4	1-5	-
PCzTh-TVDCN	26-35	39-41	-
PThTh-TVDCN	12-15	27-29	22-24

It is expected that these deviations in torsion angle, though it is generally considered that effective degree of conjugation is maintained up to torsion angles of about 40° ,³⁹ will induce changes in the oligomer electronic structures through reduction of the wave-function delocalization. To a first approximation, this can be estimated from the values of the range-separation parameters. As discussed by Körzdörfer and co-workers,³⁷ the optimized

characteristic length, $1/\omega$, of the long-range corrected density functional provides a means to examine the extent of π -conjugation.

Figure 3 shows the evolution of the characteristic length $1/\omega$ as a function of the number of repeat units. The characteristic length indeed increases with increasing chain length and then saturates at lengths of 3 to 4 repeat units, results in accordance with the behavior described by Pandey and co-workers.³⁰ However, PbTTP, and to some extent PbTBT, is an exception, as the characteristic length has not saturated after 4 repeat units. This effect can be attributed to the range-separation parameter becoming too small (*i.e.*, the functional having too little non-local Hartree-Fock exchange) for this highly conjugated, planar system.^{30, 37, 40} For the tetramers, $1/\omega$ is found to be longer in the case of the more planar systems, *e.g.*, 3.84 Å in PCzTP, 4.10 Å in PbTBT, and 4.90 Å in PbTTP. The more twisted PCzBT structure has a $1/\omega$ value of 3.23 Å while the $1/\omega$ values for the orthogonally conjugated systems PCzTh-TVDCN and PTh-TVDCN are 3.39 Å and 3.28 Å, respectively. These results are consistent with the more twisted structures having lower degrees of conjugation, which will manifest in the electronic and optical characteristics.

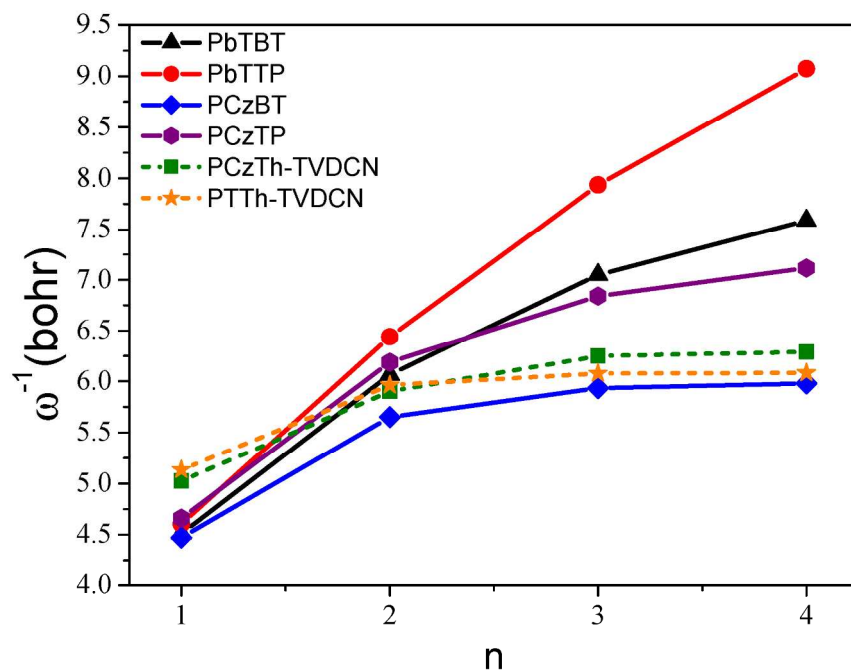


Figure 3. Characteristic length $1/\omega$ (*i.e.*, the length over which the treatment of the Coulomb operator switches from short-range to long-range), as a function of oligomer size, as determined at the tuned LC-BLYP/6-31G(d,p) level of theory.

b) HOMO and LUMO Characteristics

Figure 4 shows the evolution as a function of oligomer length, of the LC-BLYP/6-31G(d,p) HOMO and LUMO energies, which correspond in the present context to the vertical ionization potential and electron affinity values. Within the range of oligomer lengths analyzed, there is a clear linear relationship between these energies and the inverse number of repeat units. Thus, the ionization potentials for the DA copolymers are found to increase on going from PbTTP < PCzTP < PbTBT < PTTh-TVDCN < PCzTh-TVDCN < PCzBT. The smaller IPs are associated with a more coplanar configuration across the backbone, which allows for a more delocalized HOMO (see below). The electron affinities follow the trend PCzTh-TVDCN > PbTTP > PTTh-TVDCN > PbTBT > PCzTP > PCzBT. The DA tetramers with carbazole in the backbone present larger HOMO-LUMO gaps compared to the thiophene-based systems in the following order:

PCzBT (5.13 eV) > PCzTP (4.11 eV) > PTh-TVDCN (4.01 eV) > PCzTh-TVDCN (3.91 eV) > PbTBT (3.79 eV) > PbTTP (3.00 eV).

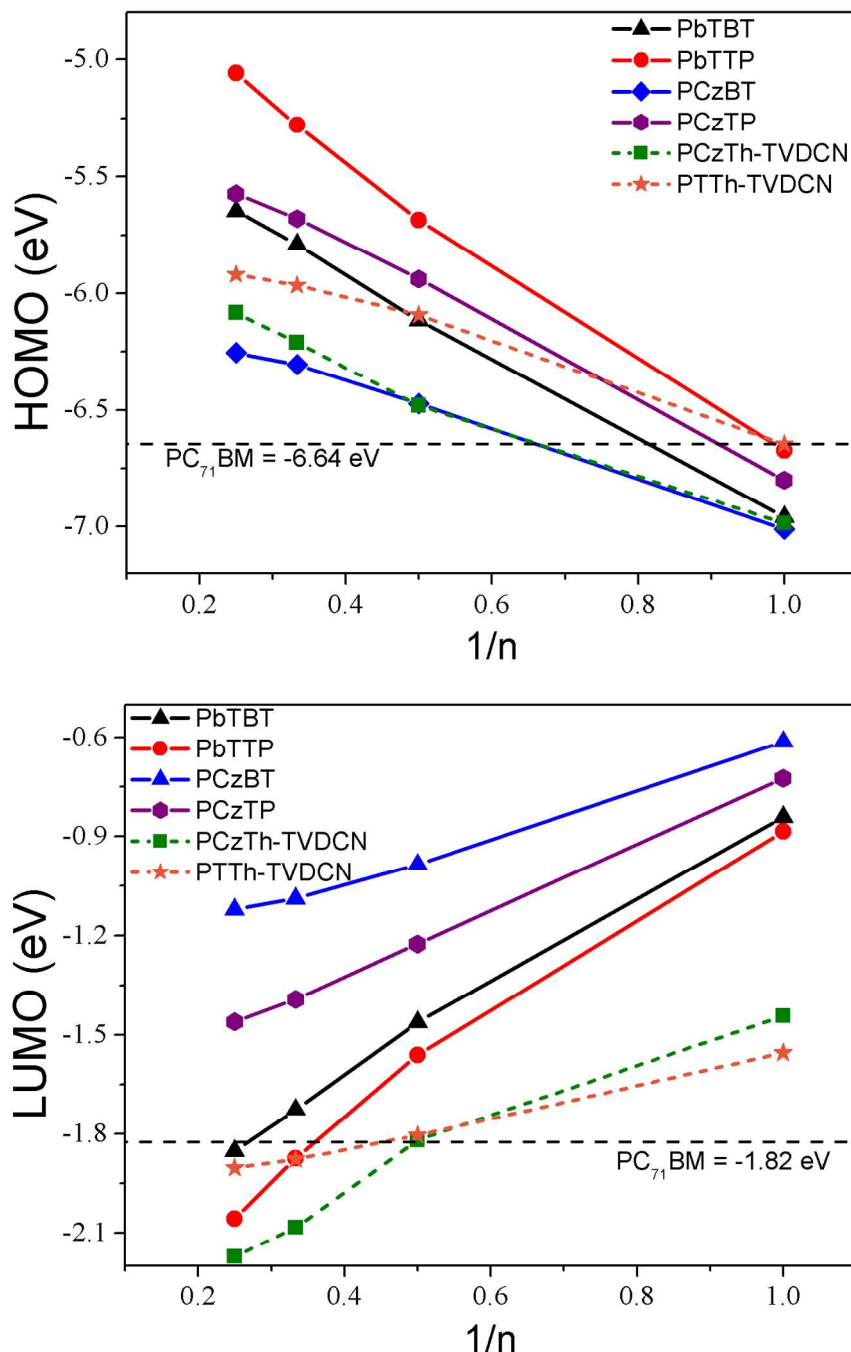


Figure 4. Evolution of the HOMO (top) and LUMO (bottom) energies (eV) with respect to the inverse number of repeat units (n) in the oligomer as determined at the tuned-LC-BLYP/6-31G(d,p) level of theory. For reference, the dashed line in each plot represents the HOMO (top) and LUMO (bottom) energy of PC₇₁BM as determined at the same level of theory.

Figure 5 illustrates the tuned LC-BLYP HOMOs and LUMOs of PbTTP and PTh-TVDCN, taken as representatives for the tetramer series. For the linear systems, the HOMOs are delocalized along the conjugated backbone; the LUMOs, on the other hand, show varying degrees of (de)localization based on the components and oligomer architecture, *e.g.*, the more coplanar backbones of PbTBT, PbTTP and PCzTP lead as expected to greater delocalization of the LUMO along the backbone as compared to the more localized LUMO on the benzothiadiazole acceptor of PCzBT. For the orthogonally conjugated systems, the HOMO is also largely delocalized along the main backbone, although to a somewhat lesser extent when compared to the linear systems; the LUMO, on the other hand, is mainly localized on the acceptor units as a result of the departure from planarity.

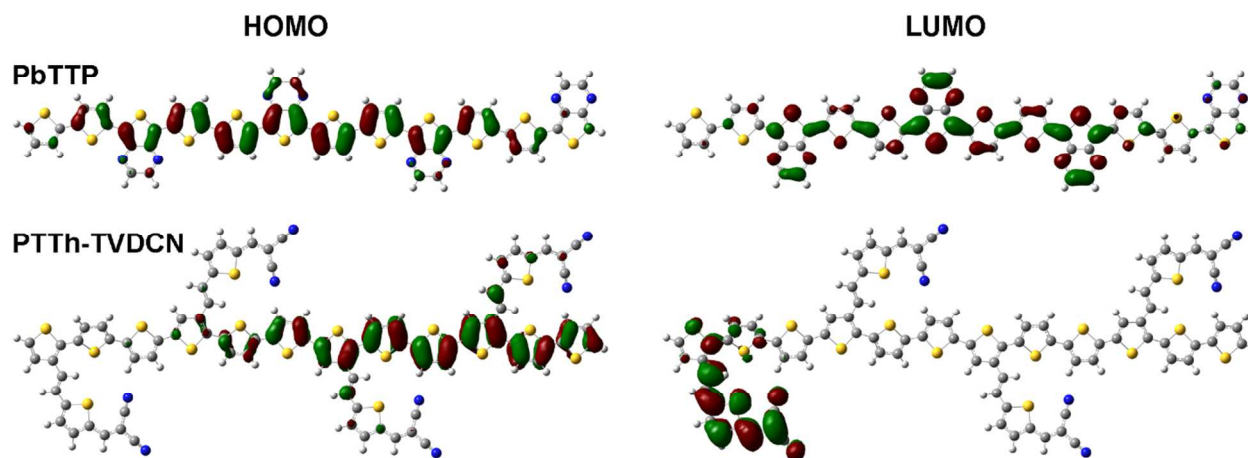


Figure 5. Illustration of the tetramer frontier molecular orbitals determined at the tuned-LC-BLYP/6-31G(d,p) level of theory.

c) Excited-State Properties and Optical Absorption

We now turn our attention to the description of the excited-state properties of these oligomers to examine how the different conjugation pathways influence optical absorption. Figure 6 shows the evolution of the $S_0 \rightarrow S_1$ vertical energies and transition dipole moments as a function of the number of repeat units as determined with TDDFT at the tuned-LC-BLYP/6-31G(d,p) level of theory. For the four linearly conjugated systems, these transitions primarily involve a HOMO \rightarrow LUMO excitation (87 to 91%); PCzBT, however, does present a more mixed transition character, as a consequence of its twisted nature. The orthogonal systems by and large show significant contributions from electronic transitions among additional frontier orbitals (see the Electronic Supplementary Information (ESI) for further details).

The $S_0 \rightarrow S_1$ transition dipole moments are predominantly aligned along the main conjugated backbone (x-axis, as defined in Figure 1) and increase in magnitude with increasing oligomer length. For PTTh-TVDCN, in addition to that along the x-axis, there is significant contribution from the y-axis component arising from the delocalization of the transition density on the orthogonally conjugated acceptor; hence, the overall transition dipole moment only weakly increases with increasing conjugation length (see ESI), a result consistent with the findings of Grimm and co-workers.²³ This result suggests that while orthogonal conjugation can lead to materials with relatively low-energy absorptions, the limited transition dipole moments – due to reduced overlap between the ground state and first excited state (see below) – will affect the efficiency of photon absorption.

The notable exception to the series is the $S_0 \rightarrow S_1$ transition dipole moment for PCzTh-TVDCN. As with PTTh-TVDCN, there is a significant delocalization of the transition density outside the

main backbone. The highly twisted nature of the structure, however, results in the transition dipole moment having non-negligible contributions coming from all three (x, y, and z) components. These transition dipole moment components, interestingly, show a differing evolution with increasing conjugation length, which results in a net decrease in transition dipole moment with increasing size for PCzTh-TVDCN.

Figure 7 collects the simulated absorption spectra where the vertical transitions are convoluted with Gaussian functions (FWHM = 0.3 eV). The positions of the vertical transitions are included to highlight the energies of the electronic states. As expected from the trends observed for the molecular orbital energies, there is a substantial bathochromic shift in the $S_0 \rightarrow S_1$ vertical transitions when going from twisted to more planar structures. Hence, a clear relationship between the characteristic length ($1/\omega$) and the $S_0 \rightarrow S_1$ energy is observed. The spectra of the linear systems can be characterized as having one dominant low-energy transition with a large oscillator strength followed by a higher-energy transition with smaller oscillator strength. For the systems with orthogonally conjugated acceptors, on the other hand, the spectra present one low-energy transition (or series of transitions) with small oscillator strength (see above) followed by a higher-energy transition with large oscillator strength. We note that the simulated spectrum for PCzTh-TVDCN is in good agreement with the experimental spectrum reported by Li and co-workers,²¹ hence providing confidence in the chosen DFT methodology to detail the intrinsic physical properties of these polymers.

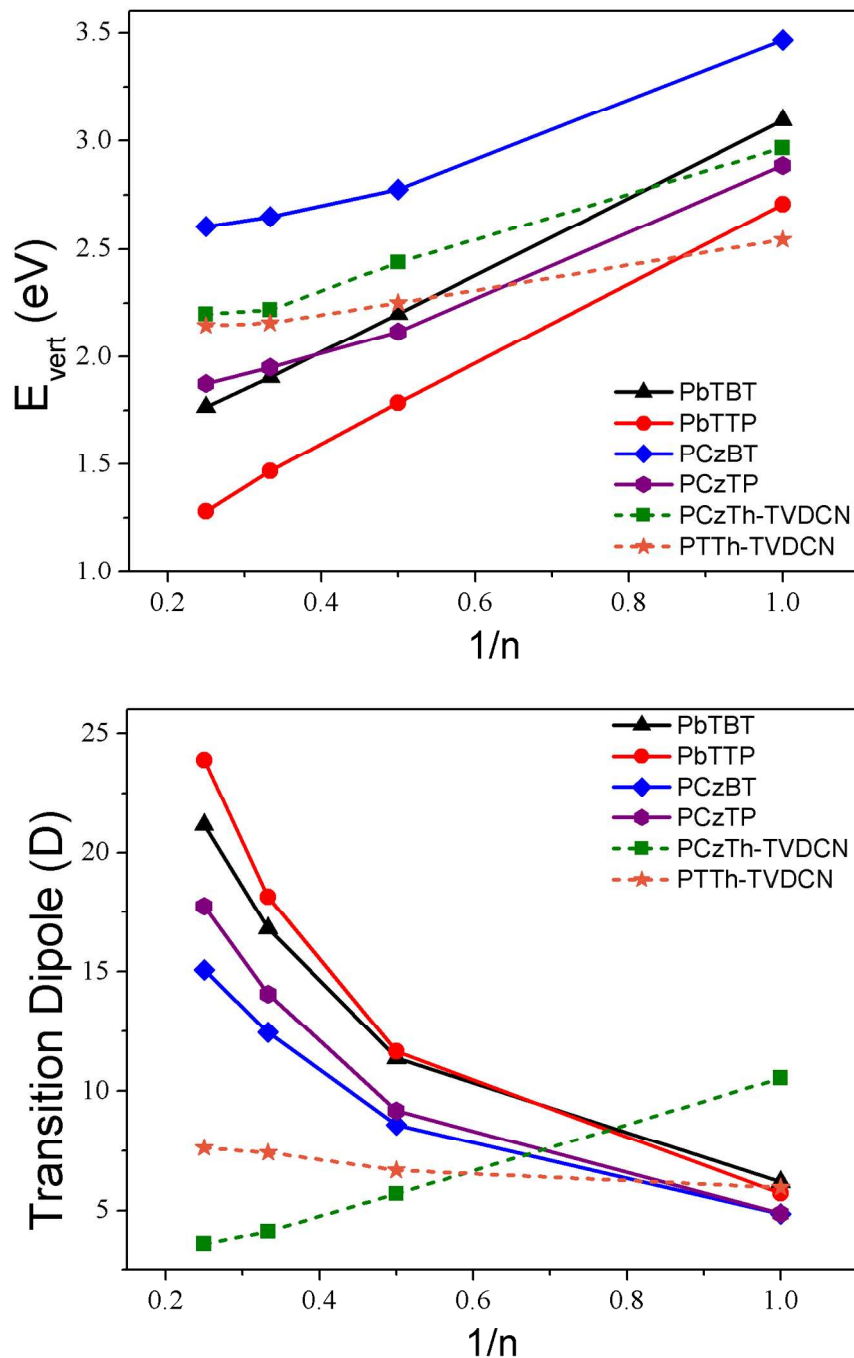


Figure 6. Evolution of the $S_0 \rightarrow S_1$ vertical transition energy (top) and absolute value of the transition dipole moment (bottom) with respect to the inverse number of repeat units ($1/n$), as calculated with TDDFT at the tuned-LC-BLYP/6-31G(d,p) level of theory.

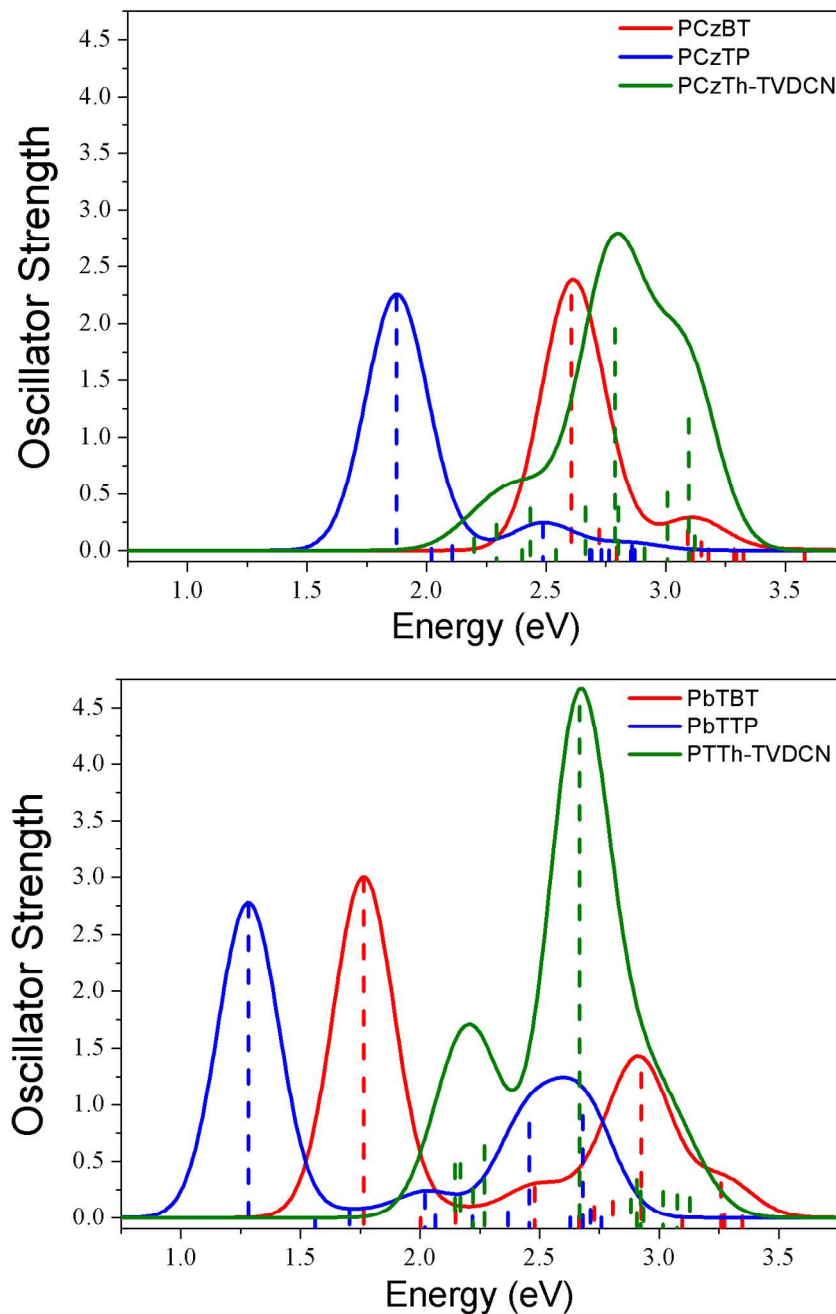


Figure 7. Simulated absorption spectra (FWHM = 0.3 eV) for the tetramers, as determined with TDDFT at the tuned-LC-BLYP/6-31G(d,p) level of theory: (top) systems with carbazole units and (bottom) systems with thiophene units along the backbone.

Natural transition orbitals (NTOs)^{4, 41} have been used to further examine the nature of absorption as there is mixing of other electronic transitions beyond HOMO→LUMO to this excitation.

Figure 8 provides representations of the NTOs and corresponding λ values (hole-particle contribution for a given electronic transition) for the $S_0 \rightarrow S_1$ transitions of representative tetramers. For the linear systems, *i.e.*, PbTBT, PbTTP, PCzBT, and PCzTP, the $S_0 \rightarrow S_1$ are predominantly HOMO→LUMO and hence the NTOs strongly resemble these orbitals (

Figure 5). For PbTBT and PbTTP, the excitation is mainly a contribution of two particle-hole pairs where both the hole and electron are largely delocalized across the conjugated backbone; in PCzTP and PCzBT, the excitation is a contribution of three particle-hole pairs where the electron tends to localize more strongly on the acceptor unit (see ESI for further details). The large spatial overlap among the hole and electron NTOs is consistent with the significant $S_0 \rightarrow S_1$ transition dipole moment in these systems.

For the orthogonally conjugated systems, the NTO for PCzTh-TVDCN is a single dominant particle-hole pair, while in PTh-TVDCN, the excitation is a contribution of two particle-hole pairs. In both cases, the hole is delocalized over the conjugated backbone and the orthogonally conjugated acceptor, while the electron is largely localized on the acceptor. Here, the limited overlap of the hole and electron NTOs reveals the reasons behind the small transition dipole moments in the lowest optical transitions of PTh-TVDCN and PCzTh-TVDCN, while pointing to the nature of the sizable transition dipole moment components orthogonal to the backbone.

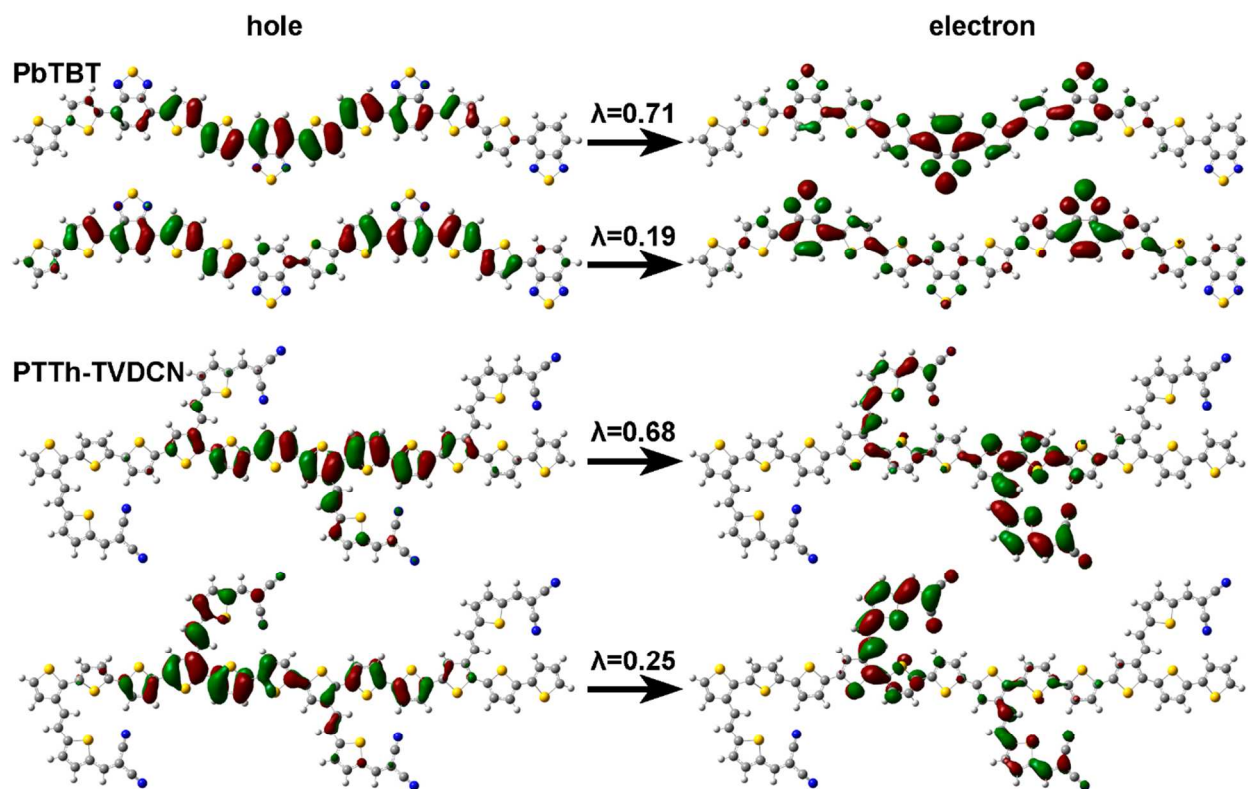


Figure 8. Illustration of the natural transition orbitals (NTO) describing the $S_0 \rightarrow S_1$ transition for the PbTBT and PTh-TVDCN tetramers as determined with TDDFT at the tuned-LC-BLYP/6-31G(d,p) level of theory; λ denotes the associated weight to the hole-particle contribution for the given electronic transition described by the NTOs.

CONCLUSION

In summary, we have used long-range-corrected density functionals to investigate a series of low optical-gap conjugated oligomers that contain benzothiadiazole and pyrazine acceptors appended in serial fashion with the donor moieties and thienylene vinylene di-cyano acceptors appended in an orthogonal manner. The system planarity, as expected, is very much influenced by the steric effects between donor and acceptor groups, even in the orthogonally conjugated case.

The value of the tuned range-separation parameter ω is confirmed to provide an effective measure of the extent of conjugation. The degree of conjugation, in turn, has significant effects on the electronic and optical properties of the systems under study. Interestingly, one of the orthogonally conjugated systems has a transition dipole moment that decreases with increasing conjugation length, a result not *a priori* expected. Our results confirm that orthogonally conjugated DA copolymers can lead to absorption into the red portion of the visible spectrum, though the transition dipole moments for these transitions should be expected to be rather limited.

Acknowledgements

ITL and DASF gratefully acknowledge the financial support from the Brazilian research agencies CAPES, CNPq and FAP-DF. The work at Georgia Tech was supported by the Deanship of Scientific Research (DSR), King Abdulaziz University, Jeddah, Saudi Arabia, under International Collaboration Grant No. D-001-433 and by the Office of Naval Research under Grant No. N00014-14-1-0171.

Electronic Supplementary Information (ESI)

Additional details provided in the electronic supplementary information (ESI) including optimized range-separation parameters for oligomers size $n=1-4$; energies and representations of frontier molecular orbitals; vertical transition energies ($S_0 \rightarrow S_1$), transition dipole moments, oscillator strengths, and corresponding electronic configurations for the DA tetramers.

Corresponding Authors

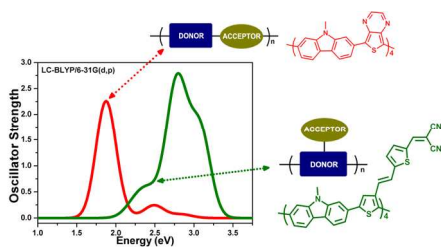
* chad.risko@uky.edu; dasf@unb.br; jean-luc.bredas@kaust.edu.sa

References

1. Y. F. Li and Y. P. Zou, *Adv Mater*, 2008, 20, 2952-2958.
2. N. Blouin, A. Michaud and M. Leclerc, *Adv Mater*, 2007, 19, 2295-2300.
3. E. Bundgaard and F. C. Krebs, *Sol Energ Mat Sol C*, 2007, 91, 954-985.
4. A. Facchetti, *Chem Mater*, 2011, 23, 733-758.
5. G. Lu, H. Usta, C. Risko, L. Wang, A. Facchetti, M. A. Ratner and T. J. Marks, *J Am Chem Soc*, 2008, 130, 7670-7685.
6. H. N. Yi, S. Al-Faifi, A. Iraqi, D. C. Watters, J. Kingsley and D. G. Lidzey, *J Mater Chem*, 2011, 21, 13649-13656.
7. J. M. Szarko, J. C. Guo, Y. Y. Liang, B. Lee, B. S. Rolczynski, J. Strzalka, T. Xu, S. Loser, T. J. Marks, L. P. Yu and L. X. Chen, *Adv Mater*, 2010, 22, 5468-5472.
8. J. H. Hou, M. H. Park, S. Q. Zhang, Y. Yao, L. M. Chen, J. H. Li and Y. Yang, *Macromolecules*, 2008, 41, 6012-6018.
9. B. Y. Fu, J. Baltazar, Z. K. Hu, A. T. Chien, S. Kumar, C. L. Henderson, D. M. Collard and E. Reichmanis, *Chem Mater*, 2012, 24, 4123-4133.
10. L. E. Polander, L. Pandey, S. Barlow, P. Tiwari, C. Risko, B. Kippelen, J. L. Bredas and S. R. Marder, *J Phys Chem C*, 2011, 115, 23149-23163.
11. L. Pandey, C. Risko, J. E. Norton and J. L. Bredas, *Macromolecules*, 2012, 45, 6405-6414.
12. T. Yasuda, Y. Sakai, S. Aramaki and T. Yamamoto, *Chem Mater*, 2005, 17, 6060-6068.
13. Z. G. Zhang, K. L. Zhang, G. Liu, C. X. Zhu, K. G. Neoh and E. T. Kang, *Macromolecules*, 2009, 42, 3104-3111.
14. E. E. Havinga, W. Tenhoeve and H. Wynberg, *Polym Bull*, 1992, 29, 119-126.
15. E. E. Havinga, W. Tenhoeve and H. Wynberg, *Synthetic Met*, 1993, 55, 299-306.
16. C. Piliego, T. W. Holcombe, J. D. Douglas, C. H. Woo, P. M. Beaujuge and J. M. J. Frechet, *J Am Chem Soc*, 2010, 132, 7595-7597.
17. Y. P. Zou, A. Najari, P. Berrouard, S. Beaupre, B. R. Aich, Y. Tao and M. Leclerc, *J Am Chem Soc*, 2010, 132, 5330-5331.
18. Y. Y. Liang and L. P. Yu, *Accounts Chem Res*, 2010, 43, 1227-1236.
19. Y. F. Li, *Accounts Chem Res*, 2012, 45, 723-733.
20. Y. P. Zou, W. P. Wu, G. Y. Sang, Y. Yang, Y. Q. Liu and Y. F. Li, *Macromolecules*, 2007, 40, 7231-7237.
21. Z. G. Zhang, H. J. Fan, J. Min, S. Y. Zhang, J. Zhang, M. J. Zhang, X. Guo, X. W. Zhan and Y. F. Li, *Polym Chem-Uk*, 2011, 2, 1678-1687.
22. P. Shen, H. J. Bin, X. W. Chen and Y. F. Li, *Org Electron*, 2013, 14, 3152-3162.
23. B. Grimm, C. Risko, J. D. Azoulay, J. L. Bredas and G. C. Bazan, *Chem Sci*, 2013, 4, 1807-1819.
24. C. T. Lee, W. T. Yang and R. G. Parr, *Phys Rev B*, 1988, 37, 785-789.
25. A. D. Becke, *Phys Rev A*, 1988, 38, 3098-3100.
26. A. D. Becke, *J Chem Phys*, 1993, 98, 5648-5652.
27. M. M. Francl, W. J. Pietro, W. J. Hehre, J. S. Binkley, M. S. Gordon, D. J. Defrees and J. A. Pople, *J Chem Phys*, 1982, 77, 3654-3665.
28. Harihara.Pc and J. A. Pople, *Theor Chim Acta*, 1973, 28, 213-222.
29. C. Risko, M. D. McGehee and J. L. Bredas, *Chem Sci*, 2011, 2, 1200-1218.

30. L. Pandey, C. Doiron, J. S. Sears and J. L. Bredas, *Phys Chem Chem Phys*, 2012, 14, 14243-14248.
31. J. D. Chai and M. Head-Gordon, *J Chem Phys*, 2008, 128.
32. A. L. Sobolewski and W. Domcke, *Chem Phys*, 2003, 294, 73-83.
33. L. Kronik, T. Stein, S. Refaely-Abramson and R. Baer, *J Chem Theory Comput*, 2012, 8, 1515-1531.
34. N. Kuritz, T. Stein, R. Baer and L. Kronik, *J Chem Theory Comput*, 2011, 7, 2408-2415.
35. R. Baer, E. Livshits and U. Salzner, *Annu Rev Phys Chem*, 2010, 61, 85-109.
36. R. Baer and D. Neuhauser, *Phys. Rev. Lett.*, 2005, 94, 043002.
37. T. Korzdorfer, J. S. Sears, C. Sutton and J. L. Bredas, *J Chem Phys*, 2011, 135, 204107.
38. J. Frisch, G. W. Trucks, H. B. Schlegel, G. E. Scuseria, M. A. Robb, J. R. Cheeseman, G. Scalmani, V. Barone, B. Mennucci, G. A. Petersson, H. Nakatsuji, M. Caricato, X. Li, H. P. Hratchian, A. F. Izmaylov, J. Bloino, G. Zheng, J. L. Sonnenberg, M. Hada, M. Ehara, K. Toyota, R. Fukuda, J. Hasegawa, M. Ishida, T. Nakajima, Y. Honda, O. Kitao, H. Nakai, T. Vreven, J. A. M. Jr, J. E. Peralta, F. Ogliaro, M. Bearpark, J. J. Heyd, E. Brothers, K. N. Kudin, V. N. Staroverov, R. Kobayashi, J. Normand, K. Raghavachari, A. Rendell, J. C. Burant, S. S. Iyengar, J. Tomasi, M. Cossi, N. Rega, J. M. Millam, M. Klene, J. E. Knox, J. B. Cross, V. Bakken, C. Adamo, J. Jaramillo, R. Gomperts, R. E. Stratmann, O. Yazyev, A. J. Austin, R. Cammi, C. Pomelli, J. W. Ochterski, R. L. Martin, K. Morokuma, V. G. Zakrzewski, G. A. Voth, P. Salvador, J. J. Dannenberg, S. Dapprich, A. D. Daniels, Ö. Farkas, J. B. Foresman, J. V. Ortiz, J. Cioslowski and a. D. J. Fox, *Gaussian Inc., Wallingford C. T.*, 2009.
39. J. L. Bredas, G. B. Street, B. Themans and J. M. Andre, *J Chem Phys*, 1985, 83, 1323-1329.
40. S. Refaely-Abramson, R. Baer and L. Kronik, *Phys Rev B*, 2011, 84, 075144.
41. R. L. Martin, *J Chem Phys*, 2003, 118, 4775-4777.

TOC Entry:



Orthogonally conjugated moieties appended to a conjugated polymer backbone are used to control solubility and packing. Here, electronic-structure calculations show how such configurations impact the polymer geometry and the electronic / optical properties.